Drastic Changes in Material Composition and Electrical Properties of Gallium-seeded Germanium Nanowires

Michael S. Seifner,[¥,‡] *Masiar Sistani,*[‖,‡] *Ivan Zivadinovic,*[¥] *Maximilian G. Bartmann,*[‖] *Alois Lugstein,*[‖] *Sven Barth**[¥,⊥]

[¥]TU Wien, Institute of Materials Chemistry, Getreidemarkt 9, 1060 Vienna, Austria.

[‖] TU Wien, Institute of Solid State Electronics, Gußhausstraße 25-25a, 1040 Vienna, Austria.

[⊥] Goethe-Universität, Physikalisches Institut, Max-von-Laue-Straße 1, 60438 Frankfurt am Main, Germany.

*Corresponding author: S. Barth, E-mail: sven.barth@tuwien.ac.at; barth@physik.uni-frankfurt.de Fax: +43 158801 165 99; Tel: +43 158801 165 207

ABSTRACT.

Varying the growth conditions of gallium seeded germanium nanostructures leads to significant variations in morphology and particularly of the electronic properties inducing a transition from the hyperdoping regime to intrinsic germanium crystal formation. The consumption of the growth seed leads to nanocones with incorporation of ~3.8±0.7 at% Ga at temperatures below 350 °C while a high density of Ge nanowires with constant diameter can be obtained at higher temperatures. The high temperature Ga-seeded Ge nanowires exhibit electronic properties of intrinsic Ge nanowires.

KEYWORDS. germanium; nanowires; hyperdoping; gallium; semiconductor

Ge nanowires (NWs) have demonstrated their potential for different applications including field effect transistors,[1] lithium ion batteries,[2] solar cells[3] and humidity sensors.[4] A wide range of bottom-up and top-down approaches have been successfully applied to prepare Ge NWs.[5] Among the large variety of preparation techniques, metal-assisted, bottom-up growth is the most popular approach to obtain Ge NWs with smooth side walls and tunable diameters. More specifically, different metallic growth seeds have been identified to facilitate the formation of highly crystalline Ge NWs, while the temperature window of their activity to serve as nucleation seed varies.[6-8] In addition to the morphological control, the implementation of these nanostructures in device architectures as well as the actual suitability of a semiconductor NW often requires a doping of the Ge crystal, which is typically achieved *in situ* during crystal growth.[9-11] In the recent past, the incorporation of dopants in the Ge host lattice has been in the focus of several studies. For instance, the effective doping of Ge nanostructures with group III atoms as p-dopants has been observed in low temperature synthesis using Ga, In, and Bi. [12-13 14] Especially the incorporation of high Ga percentage in anisotropic Ge crystals via a low temperature chemical vapor deposition,[12] thermally induced liquid-based crystal growth[15] and electrodeposition using Ga electrodes[16-18] was described to result in homogeneously distributed dopants that are electronically active. The use of a metal acting as a crystal growth promoter and an incorporation in the wire material in large quantities to obtain a binary compound can be described as a modified version of a self-seeding mechanism. This technique of using a metal particle as an efficient source of a component was first described for Ga- and In-based III-V semiconductor nanowire growth.[19-21] Adapting this method allows the formation of metastable materials at low temperature by incorporation of the seed material in the growing Ge lattice in the percent range and thus altering the physical properties of the material dramatically.[12, 22-24]

We report two regimes for anisotropic Ge crystal growth using Ga as metallic seeds. Low temperatures < 350 °C result in an effective incorporation of Ga into the NW during the growth, which can be associated with Ga-hyperdoping. Higher temperatures above 360 °C prevent the integration of Ga in the growing semiconductor crystal. The resistivity values of the Ga-seeded Ge NWs ($1.5 \cdot 10^{-2}$ Ωm) are comparable with intrinsic Au-seeded Ge NWs ($8.8 \cdot 10^{-3}$ Ωm) and an increase by 6 orders of magnitude upon cooling from room temperature to 10 K is observed. Two-terminal devices with Al as contact material show typical Schottky field effect transistor (FET) behavior with ambipolar switching but suggest weak p-type behavior that can be caused by trap states at the surface and metal-semiconductor interface.

RESULTS AND DISCUSSION

Nanostructures presented in this study are exclusively prepared in a two-step preparation method. First Ga seeds are formed by thermal decomposition of $Ga(N(CH_3)_2)_2$ in toluene at 350 °C. Subsequently the Ge nanostructures are grown by liquid injection CVD using diphenylgermane (DPG) diluted in toluene at temperatures between 300-400 °C. Figure 1a shows a typical scanning electron microscopy (SEM) image of Ga-seeded Ge crystal growth at 340 °C illustrating the consumption of the Ga particle. The shrinking diameter of the crystal with length is a common feature when the metallic growth seed is consumed during growth.[22, 25] A scanning transmission electron microscopy energy dispersive X-ray spectroscopy (STEM-EDX) map for Ga and Ge is shown in the inset of Figure 1a. The Ga seed at the NW tip is located on top of the tapered NW indicating the aforementioned incorporation mechanism associated with catalyst consumption resulting in nanocone morphologies. The cone structures are highly crystalline according to the high resolution transmission electron microscopy (TEM) image in Figure 1b and the growth direction can be assigned to be along the ⟨111⟩-direction as illustrated

in the corresponding fast Fourier transformation (FFT) image. The Ga content is in the range of ~3.8±0.7 at% for different Ge nanocones and homogeneously distributed within the Ge crystal matrix as shown in Figure 1c. This Ga content is close to the previously published Ga-hyperdoped Ge NWs prepared in the temperature range of 210-230 °C.[12] Therefore, similar solute trapping mechanism of Ga at step edges during the Ge NW growth is expected even at >100 °C higher temperatures as described in the previous study. The efficiency of Ga incorporation can be also a consequence of the similar atomic radii of Ga and Ge and thus an absence of strain by the incorporation of the metal in the semiconductor lattice.[26] The solute trapping model has been discussed in literature for the incorporation of unusually high Al contents in Si NWs and should be valid also in this case.[27-28] The high Ga concentration trapped in the Ge matrix represents a metastable material composition as described in literature and illustrated by STEM-EDX showing a clustering of Ga during annealing at 400 °C.[12]

In contrast to cone-like structures observed at temperatures <350 °C, a high density of Ge NWs with constant diameter can be obtained by increasing the synthesis temperature to ~400 °C during the CVD growth using DPG. No notable tapering is discernible in these NWs and their diameter is usually in the range of 10-20 nm while typical lengths are several micrometers as shown in the SEM image in Figure 2a. High resolution TEM shows highly crystalline Ge. The Fast Fourier Transformation (FFT) pattern shown in the inset depicts the growth direction of the Ge NWs to be along the ⟨110⟩-axis, which is the typical orientation for group IV NWs of this small diameter regime.[29-30] The ⟨110⟩ growth direction of small diameter group IV NWs has been attributed to energy contributions of side facets;[31-32] however, the contributions of side-wall adsorption of decomposition products cannot be ruled out and variations of adsorbates on side facets have been described to cause changes in growth direction.[33-35] Therefore, the changes in

growth direction with temperature cannot be assigned unequivocally to size effects, even though the same DPG precursor results in different preferred growth directions upon changes in NW diameter.[30]

EDX-maps for these NWs do not show any preferential Ga incorporation in the NWs (Figure 2c). A significant consumption of Ga due to the incorporation in the Ge lattice, which would be associated with decreasing diameter as discussed above, was not expected from SEM images either showing constant Ge NW diameter for several tens of nanometers (Figure 2a). However, given the resolution limit of EDX of ~0.5 at% an incorporation of a low Ga concentration cannot be excluded by this technique and the determination of activated dopants via the electronic properties can be used to gain further knowledge.

The electronic properties of Ga-seeded Ge NWs grown at higher temperatures of ~400 °C have been determined. Devices of individual NWs have been prepared by drop-casting NWs from an isopropanol solution on Si substrates with a 100 nm thick, thermally grown SiO_2 layer. The Ge NWs have been contacted by aluminum pads fabricated by electron-beam lithography, sputter deposition, and lift-off techniques. Two-terminal *I*/*V* measurements of Ga-seeded Ge NWs show typical back-to-back Schottky contacts and significant influence of the contact resistance. Four-terminal measurements are used to exclude the contact resistances and related I/V curves are shown in Figure 3a. The resistivity values determined from four-terminal devices are $1.5 \cdot 10^{-2}$ Ωm for Ga-seeded Ge NWs and $8.8 \cdot 10^{-3}$ Ωm for the Au-seeded Ge NWs at room temperature. These results illustrate that the Ga-seeded Ge NWs are behaving like intrinsic Ge and not like the previously described CVD-grown Ga-hyperdoped $Ge_{0.97}Ga_{0.03}$ NWs with a resistivity of $3 \cdot 10^{-6}$ Ωm[12] and electrochemically prepared $Ge_{0.9}Ga_{0.1}$ microwires ~410^{-4} Ωm.[18] The temperature dependence of resistivity is shown in Figure 3b illustrating a change of six orders of magnitude

upon cooling from 300 to 4 K mirroring the Au-seeded NWs electronic behavior. In contrast, the $Ge_{0.97}Ga_{0.03}$ NW grown in the low temperature region exhibit a weakly metallic-like temperature-dependent resistivity.[12]

The transition from hyperdoping with significant Ga incorporation to a material with the characteristics of intrinsic Ge is first and foremost attributed to the higher temperatures used during the crystal growth. This thermodynamic effect could either facilitate Ga diffusion of potentially trapped atoms back into the Ga metal seed or prevent the incorporation due to the high covalency of the Ge crystal. Moreover, a diameter-dependence for the incorporation of Ga atoms at substitutional sites in Ge should not be neglected and cannot be excluded. Diameter-dependent dopant location has been described in literature for Si NWs, illustrating a transition from NW-bulk doping to a surface enrichment for diameters in the range of ~20 nm.[36] This is very close to the Ge NW diameter observed in the here presented study. Considering the high mobility of Ga and its tendency of diffusion at elevated temperatures, these atoms could be recollected at the growth front by surface diffusion or a very small number of Ga atoms at the surface layer could be deactivated by post-growth oxidation. The exact reason for this peculiar effect of Ga incorporation inefficiency is not clear yet. Models describing the self-cleaning of semiconductor nanocrystals and doping limits depending on the crystal size usually refer to crystal sizes below 5 nm in diameter which is much small than in the here described NWs.[37-38] In addition, the type of doping in a semiconductor material and the growth temperature have significant influence on the critical diameter.[39] Several factors can influence the composition of a doped crystal including the general crystal growth kinetics, time between layer nucleation events in a step-flow growth model associated with the impurity trapping mechanism of NW growth.[40-41] To date, information about the interface between the Ga metal seed and the forming Ge crystal

under growth conditions, which could be a tilted (111) or a horizontal (110) Ge facet,[31] is currently missing and could provide further insight in potential influences on the material composition.[31] An indication on the potential diameter influence on the composition could be observed in individual cases, where a transition from cone to a NW structure with a constant diameter was evident. These structures showing both regimes have been obtained at growth temperatures close to 350 °C as shown in Figure S1 of the supplementary information. For typical cone-type structures there is no indication of a diameter-dependent Ga incorporation efficiency towards the tip section and the Ga content remains constant for diameters down to 20 nm in the tip region (Figure S2).

Although the *I/V* measurements as well as the temperature dependence of resistivity show the characteristic of intrinsic Ge NWs, according to negative surface charges accumulating in interband trap levels,[42] a weak overall p-type behavior of the NWs was observed (Figure 4). The conductivity in the channel can be altered by applying a back-gate voltage modulating the charge carrier concentration and shifting the Fermi level of the Ge NW. Considering the sweep from negative to positive gate-voltage (red line), at V_G = -2 V the current through the NW reaches its minimum. Thus, in a simplified model (i.e. no barriers at the contacts and no band bending across the NW) it can be assumed that the conductivity at this point of the transfer characteristic corresponds to the conductivity of the intrinsic semiconductor.[10] By decreasing $V_{G,}$ a higher current through the channel is recorded due to a shift of the Fermi level towards the valence band, which increases the hole concentration and thus conductivity of the Ge NW. In contrast, for an increase of V_G beyond V_G = -2 V, inversion takes place and a transition from hole to electron dominated transport regime is observed. This ambipolar behavior is a common property observed in semiconductor NWs.[43] The measurements further reveal a highly reproducible

hysteresis for changing the sweep-direction of the transfer characteristic. According to the large surface-to-volume ratio of the Ge NWs, this is attributed to kinetic effects, mostly related to charge- carrier trapping at the surface.[42, 44] Concluding, the high resistivity values and ambipolar behavior are a clear indication of intrinsic nature of the Ga seeded Ge NWs grown at high temperatures.

CONCLUSION

We demonstrate a transition from a regime of Ga hyperdoping to the formation of intrinsic Ge NWs using Ga-seeded growth of Ge NWs at temperatures of 300-400 °C. In contrast to hyperdoped Ge, the Ga-seeded Ge NWs in the high temperature region do not show any Ga incorporation in EDX maps nor a p-type doping in electrical characterization. The transfer characteristics resemble intrinsic Ge NWs with resistivities in the range of $1.5 \cdot 10^{-2}$ Ωm at room temperature and an increase by six orders of magnitude upon cooling to 10 K. Moreover, typical ambipolar behavior of a Schottky FET has been observed using single NW devices.

METHODS

All synthetic procedures and handling of the chemicals for the nanostructure synthesis have been carried out using Schlenk techniques or an argon-filled glove box (MBraun). Solvents have been dried over sodium and stored in a glove box. The tris(dimenthylamido)gallium(III) precursor ($Ga(N(CH_3)_2)_3$) was prepared using $GaCl_3$ and $LiN(CH_3)_2$ for a salt elimination according to literature[45] and sublimed at 55 °C (10^{-3} mbar). Diphenyl-butylgermane (DPG) was purchased from ABCR.

Nanostructure synthesis.

Nanowire growth. The experiments have been conducted in a 5 ml cell in a flow through configuration using tubing and gauges from HiP High Pressure Equipment. The reaction vessel was loaded with a Si collector substrate and dried over night under dynamic vacuum at 120 °C. After cooling, the vessel was filled with 4 ml toluene and 1 mg $Ga(N(CH_3)_2)_3$ and closed. The vessel was heated up to 350 °C in a pre-heated tube furnace for 1h to decompose the Ga precursor and form metallic Ga. After 1h, the pressurized cell is slowly opened to remove the toluene and by-products of the $Ga(N(CH_3)_2)_3$ decomposition. The closed system was heated to the desired decomposition temperature of DPG (300-400 °C), stabilized for 15 min and the injection of 2 mL DPG in toluene (10 mg/mL) was started using a syringe pump with an injection rate 1 – 1,5 mL/h while the outlet tab was also opened. After the injection of precursor, the reaction vessel was closed on both ends and cooled to room temperature.

Nanostructure characterization. The Ga-seeded Ge NWs and nanocones were analyzed using a FEI Inspect F50 scanning electron microscope (SEM). In this study, a FEI TECNAI F20 operated at 200 kV and equipped with high angle annular dark field (HAADF) STEM and EDX detector was used. The limited accuracy of the EDX analysis can lead to a potential deviation by ±0.5 at% of the values stated in the manuscript. The elemental maps were recorded and quantified using the AMETEK TEAM package. The images were recorded and treated using Digital Micrograph software.

Electrical characterization. The vapor-grown Ge NWs have been deposited by drop-casting of a NW suspension in isopropanol onto a highly p-doped Si substrate with a 100 nm thick,

thermally grown SiO_2 layer and predefined macroscopic Ti-Au bonding pads. Individual NWs have been contacted with 100 nm thick Al pads by electron beam lithography, Al sputter deposition preceded by a HI dip, and lift-off techniques.

The electrical measurements at room-temperature and ambient conditions were performed using a combination of a semiconductor analyzer (HP 4156B) and a probe station. To minimize the influence of ambient light as well as electromagnetic fields, the probe station was placed in a dark box. Low-temperature measurements (10-300 K) were performed in vacuum at a pressure of approximately 2.5×10^{-5} mbar using a ^{4}He cryostat (Cryo Industries CRC-102) and a semiconductor analyzer (Keysight B1500A).

ASSOCIATED CONTENT

Supporting Information. TEM image of a Ga-hyperdoped Ge nanocone with transition to a Ge NW with constant diameter and STEM-EDX maps of the termination region in a cone-type structure.

AUTHOR INFORMATION

Corresponding Author

* S. Barth, E-mail: sven.barth@tuwien.ac.at; Fax: +43 158801 165 99; Tel: +43 158801 165 207

Author Contributions

‡These authors contributed equally. The manuscript was written through contributions of all authors. All authors have given approval to the final version of the manuscript.

Funding Sources

This work was funded by the Fonds zur Förderung der Wissenschaftlichen Forschung (FWF), Austria (project P 28524). Parts of this study were funded by the Deutsche Forschungsgemeinschaft (DFG, German Research Foundation) – 413940754.

ACKNOWLEDGMENT

We thank University Service Center for TEM (USTEM) for access to the electron microscopes at TU Wien. This work was funded by the Fonds zur Förderung der Wissenschaftlichen Forschung (FWF), Austria (project P 28524). S.B. thanks for funding by the Deutsche Forschungsgemeinschaft (DFG, German Research Foundation) – 413940754.

REFERENCES

1. Wang, D.; Wang, Q.; Javey, A.; Tu, R.; Dai, H.; Kim, H.; McIntyre, P. C.; Krishnamohan, T.; Saraswat, K. C., Germanium Nanowire Field-Effect Transistors with SiO2 and High-κ HfO2 Gate Dielectrics. *Appl. Phys. Lett.* **2003,** *83*, 2432-2434.
2. Kennedy, T.; Mullane, E.; Geaney, H.; Osiak, M.; O'Dwyer, C.; Ryan, K. M., High-Performance Germanium Nanowire-Based Lithium-Ion Battery Anodes Extending over 1000 Cycles Through *in Situ* Formation of a Continuous Porous Network. *Nano Lett.* **2014,** *14*, 716-723.
3. Yun, J.-H.; Park, Y. C.; Kim, J.; Lee, H.-J.; Anderson, W. A.; Park, J., Solution-Processed Germanium Nanowire-Positioned Schottky Solar Cells. *Nanoscale Res. Lett.* **2011,** *6*, 287.
4. Samà, J.; Seifner, M. S.; Domènech-Gil, G.; Santander, J.; Calaza, C.; Moreno, M.; Gràcia, I.; Barth, S.; Romano-Rodríguez, A., Low temperature humidity sensor based on Ge nanowires selectively grown on suspended microhotplates. *Sens. Actuator B-Chem.* **2017,** *243*, 669-677.
5. Barth, S.; Hernandez-Ramirez, F.; Holmes, J. D.; Romano-Rodriguez, A., Synthesis and Applications of One-Dimensional Semiconductors. *Prog. Mater. Sci.* **2010,** *55*, 563-627.
6. Lensch-Falk, J. L.; Hemesath, E. R.; Perea, D. E.; Lauhon, L. J., Alternative Catalysts for VSS Growth of Silicon and Germanium Nanowires. *J. Mater. Chem.* **2009,** *19*, 849-857.
7. O'Regan, C.; Biswas, S.; Petkov, N.; Holmes, J. D., Recent Advances in the Growth of Germanium Nanowires: Synthesis, Growth Dynamics and Morphology Control. *J. Mater. Chem. C* **2014,** *2*, 14-33.
8. Seifner, M. S.; Pertl, P.; Bernardi, J.; Biswas, S.; Holmes, J. D.; Barth, S., Lead-Supported Germanium Nanowire Growth. *Mater. Lett.* **2016,** *173*, 248-251.

9. Perea, D. E.; Hemesath, E. R.; Schwalbach, E. J.; Lensch-Falk, J. L.; Voorhees, P. W.; Lauhon, L. J., Direct Measurement of Dopant Distribution in an Individual Vapour-Liquid-Solid Nanowire. *Nat. Nanotechnol.* **2009,** *4*, 315-319.
10. Zhang, S.; Hemesath, E. R.; Perea, D. E.; Wijaya, E.; Lensch-Falk, J. L.; Lauhon, L. J., Relative Influence of Surface States and Bulk Impurities on the Electrical Properties of Ge Nanowires. *Nano Lett.* **2009,** *9*, 3268-3274.
11. Tutuc, E.; Chu, J. O.; Ott, J. A.; Guha, S., Doping of Germanium Nanowires Grown in Presence of PH3. *Appl. Phys. Lett.* **2006,** *89*, 3.
12. Seifner, M. S.; Sistani, M.; Porrati, F.; Di Prima, G.; Pertl, P.; Huth, M.; Lugstein, A.; Barth, S., Direct Synthesis of Hyperdoped Germanium Nanowires. *ACS Nano* **2018,** *12*, 1236-1241.
13. Aghazadeh Meshgi, M.; Biswas, S.; McNulty, D.; O'Dwyer, C.; Alessio Verni, G.; O'Connell, J.; Davitt, F.; Letofsky-Papst, I.; Poelt, P.; Holmes, J. D.; Marschner, C., Rapid, Low-Temperature Synthesis of Germanium Nanowires from Oligosilylgermane Precursors. *Chem. Mater.* **2017,** *29*, 4351–4360.
14. Tabatabaei, K.; Lu, H.; Nolan, B. M.; Cen, X.; McCold, C. E.; Zhang, X.; Brutchey, R. L.; van Benthem, K.; Hihath, J.; Kauzlarich, S. M., Bismuth Doping of Germanium Nanocrystals through Colloidal Chemistry. *Chem. Mater.* **2017,** *29*, 7353-7363.
15. Pertl, P.; Seifner, M. S.; Herzig, C.; Limbeck, A.; Sistani, M.; Lugstein, A.; Barth, S., Solution-Based Low-Temperature Synthesis of Germanium Nanorods and Nanowires. *Monatsh. Chem.* **2018,** 1345-1350.
16. Fahrenkrug, E.; Gu, J.; Jeon, S.; Veneman, P. A.; Goldman, R. S.; Maldonado, S., Room-Temperature Epitaxial Electrodeposition of Single-Crystalline Germanium Nanowires at the Wafer Scale from an Aqueous Solution. *Nano Lett.* **2014,** *14*, 847-852.
17. Fahrenkrug, E.; Biehl, J.; Maldonado, S., Electrochemical Liquid–Liquid–Solid Crystal Growth of Germanium Microwires on Hard and Soft Conductive Substrates at Low Temperature in Aqueous Solution. *Chem. Mater.* **2015,** *27*, 3389-3396.
18. Acharya, S.; Ma, L.; Maldonado, S., Critical Factors in the Growth of Hyperdoped Germanium Microwires by Electrochemical Liquid–Liquid–Solid Method. *ACS Appl. Nano Mater.* **2018,** *1*, 5553-5561.
19. Novotny, C. J.; Yu, P. K. L., Vertically Aligned, Catalyst-Free InP Nanowires Grown by Metalorganic Chemical Vapor Deposition. *Appl. Phys. Lett.* **2005,** *87*, 203111.
20. Colombo, C.; Spirkoska, D.; Frimmer, M.; Abstreiter, G.; Fontcuberta i Morral, A., Ga-assisted catalyst-free growth mechanism of GaAs nanowires by molecular beam epitaxy. *Phys. Rev. B* **2008,** *77*, 155326.
21. Dubrovskii, V. G.; Xu, T.; Álvarez, A. D.; Plissard, S. R.; Caroff, P.; Glas, F.; Grandidier, B., Self-Equilibration of the Diameter of Ga-Catalyzed GaAs Nanowires. *Nano Lett.* **2015,** *15*, 5580-5584.
22. Seifner, M. S.; Biegger, F.; Lugstein, A.; Bernardi, J.; Barth, S., Microwave-Assisted $Ge_{1-x}Sn_x$ Nanowire Synthesis: Precursor Species and Growth Regimes. *Chem. Mater.* **2015,** *27*, 6125-6130.
23. Sistani, M.; Seifner, M. S.; Bartmann, M. G.; Smoliner, J.; Lugstein, A.; Barth, S., Electrical Characterization and Examination of Temperature-Induced Degradation of Metastable $Ge_{0.81}Sn_{0.19}$ Nanowires. *Nanoscale* **2018,** *10*, 19443-19449.

24. Seifner, M. S.; Hernandez, S.; Bernardi, J.; Romano-Rodriguez, A.; Barth, S., Pushing the Composition Limit of Anisotropic $Ge_{1-x}Sn_x$ Nanostructures and Determination of Their Thermal Stability. *Chem. Mater.* **2017,** *29*, 9802-9813.
25. Ermez, S.; Jones, E. J.; Crawford, S. C.; Gradečak, S., Self-Seeded Growth of GaAs Nanowires by Metal–Organic Chemical Vapor Deposition. *Cryst. Growth Des.* **2015,** *15*, 2768-2774.
26. Cordero, B.; Gomez, V.; Platero-Prats, A. E.; Reves, M.; Echeverria, J.; Cremades, E.; Barragan, F.; Alvarez, S., Covalent Radii Revisited. *Dalton Trans.* **2008,** 2832-2838.
27. Moutanabbir, O.; Isheim, D.; Blumtritt, H.; Senz, S.; Pippel, E.; Seidman, D. N., Colossal Injection of Catalyst Atoms into Silicon Nanowires. *Nature* **2013,** *496*, 78-82.
28. Moutanabbir, O.; Senz, S.; Scholz, R.; Alexe, M.; Kim, Y.; Pippel, E.; Wang, Y.; Wiethoff, C.; Nabbefeld, T.; Meyer zu Heringdorf, F.; Horn-von Hoegen, M., Atomically Smooth p-Doped Silicon Nanowires Catalyzed by Aluminum at Low Temperature. *ACS Nano* **2011,** *5*, 1313-1320.
29. Schmidt, V.; Senz, S.; Gosele, U., Diameter-Dependent Growth Direction of Epitaxial Silicon Nanowires. *Nano Lett.* **2005,** *5*, 931-935.
30. Barth, S.; Koleśnik, M. M.; Donegan, K.; Krstić, V.; Holmes, J. D., Diameter-Controlled Solid-Phase Seeding of Germanium Nanowires: Structural Characterization and Electrical Transport Properties. *Chem. Mater.* **2011,** *23*, 3335-3340.
31. Hanrath, T.; Korgel, B. A., Crystallography and surface faceting of germanium nanowires. *Small* **2005,** *1*, 717-721.
32. Wu, Y.; Cui, Y.; Huynh, L.; Barrelet, C. J.; Bell, D. C.; Lieber, C. M., Controlled growth and structures of molecular-scale silicon nanowires. *Nano Lett.* **2004,** *4*, 433-436.
33. Shin, N.; Filler, M. A., Controlling Silicon Nanowire Growth Direction via Surface Chemistry. *Nano Lett.* **2012,** *12*, 2865-2870.
34. Kolíbal, M.; Pejchal, T.; Vystavěl, T.; Šikola, T., The Synergic Effect of Atomic Hydrogen Adsorption and Catalyst Spreading on Ge Nanowire Growth Orientation and Kinking. *Nano Lett.* **2016,** *16*, 4880-4886.
35. Sivaram, S. V.; Shin, N.; Chou, L.-W.; Filler, M. A., Direct Observation of Transient Surface Species during Ge Nanowire Growth and Their Influence on Growth Stability. *Journal of the American Chemical Society* **2015,** *137*, 9861-9869.
36. Xie, P.; Hu, Y.; Fang, Y.; Huang, J.; Lieber, C. M., Diameter-Dependent Dopant Location in Silicon and Germanium Nanowires. *Proc. Natl. Acad. Sci. U.S.A.* **2009,** *106*, 15254-15258.
37. Chan, T. L.; Tiago, M. L.; Kaxiras, E.; Chelikowsky, J. R., Size Limits on Doping Phosphorus into Silicon Nanocrystals. *Nano Lett.* **2008,** *8*, 596-600.
38. Dalpian, G. M.; Chelikowsky, J. R., Self-Purification in Semiconductor Nanocrystals. *Physical Review Letters* **2006,** *96*, 226802.
39. Khanal, D. R.; Yim, J. W. L.; Walukiewicz, W.; Wu, J., Effects of Quantum Confinement on the Doping Limit of Semiconductor Nanowires. *Nano Lett.* **2007,** *7*, 1186-1190.
40. Gamalski, A. D.; Ducati, C.; Hofmann, S., Cyclic Supersaturation and Triple Phase Boundary Dynamics in Germanium Nanowire Growth. *The Journal of Physical Chemistry C* **2011,** *115*, 4413-4417.
41. Wen, C. Y.; Tersoff, J.; Reuter, M. C.; Stach, E. A.; Ross, F. M., Step-Flow Kinetics in Nanowire Growth. *Phys. Rev. Lett.* **2010,** *105*, 195502.

42. Hanrath, T.; Korgel, B. A., Influence of Surface States on Electron Transport through Intrinsic Ge Nanowires. *J. Phys. Chem. B* **2005,** *109*, 5518-5524.
43. Byon, K.; Tham, D.; Fischer, J. E.; Johnson, A. T., Systematic Study of Contact Annealing: Ambipolar Silicon Nanowire Transistor with Improved Performance. *Appl. Phys. Lett.* **2007,** *90*, 143513.
44. Fujii, H.; Kanemaru, S.; Matsukawa, T.; Itoh, J., Air-Bridge-Structured silicon Nanowire and Anomalous Conductivity. *Appl. Phys. Lett.* **1999,** *75*, 3986-3988.
45. Yarema, M.; Wörle, M.; Rossell, M. D.; Erni, R.; Caputo, R.; Protesescu, L.; Kravchyk, K. V.; Dirin, D. N.; Lienau, K.; von Rohr, F.; Schilling, A.; Nachtegaal, M.; Kovalenko, M. V., Monodisperse Colloidal Gallium Nanoparticles: Synthesis, Low Temperature Crystallization, Surface Plasmon Resonance and Li-Ion Storage. *J. Am. Chem. Soc.* **2014,** *136*, 12422-12430.

For Table of Contents Use Only

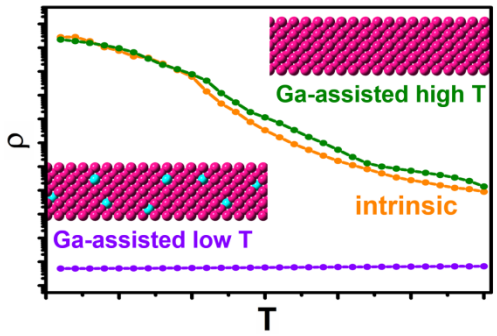

Synopsis:

Significant morphological and compositional changes have been observed for Ga-seeded Ge nanocrystal growth. Moreover, the electronic properties show a transition from the hyperdoping regime to intrinsic germanium for anisotropic crystals grown at different temperatures.

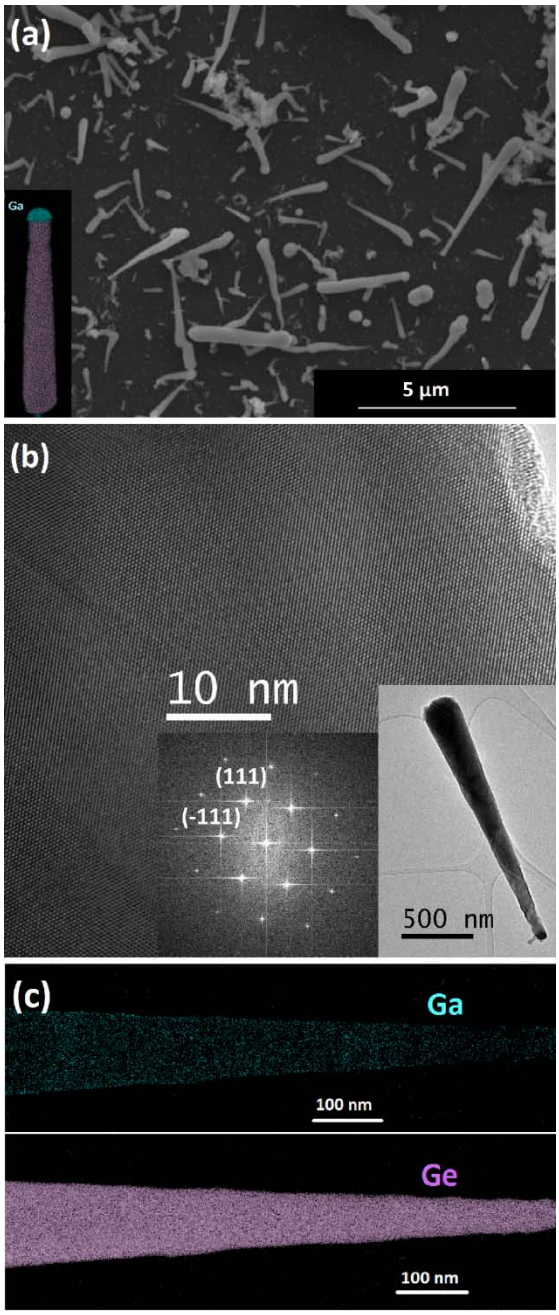

Figure 1. (a) SEM image shows Ge nanostructures with diminishing diameter along their length grown from Ga seeds at 340 °C. The STEM-EDX map overlay in the inset illustrates that the Ga seed is located on the side with smaller diameter during the growth. (b) High-resolution TEM image reveals a high crystallinity of the Ge crystal and a ⟨111⟩ growth direction of the cone-type nanostructures from thick to thin extreme. The STEM-EDX maps for Ga and Ge in (c) illustrate a homogeneous distribution of Ga in the crystal.

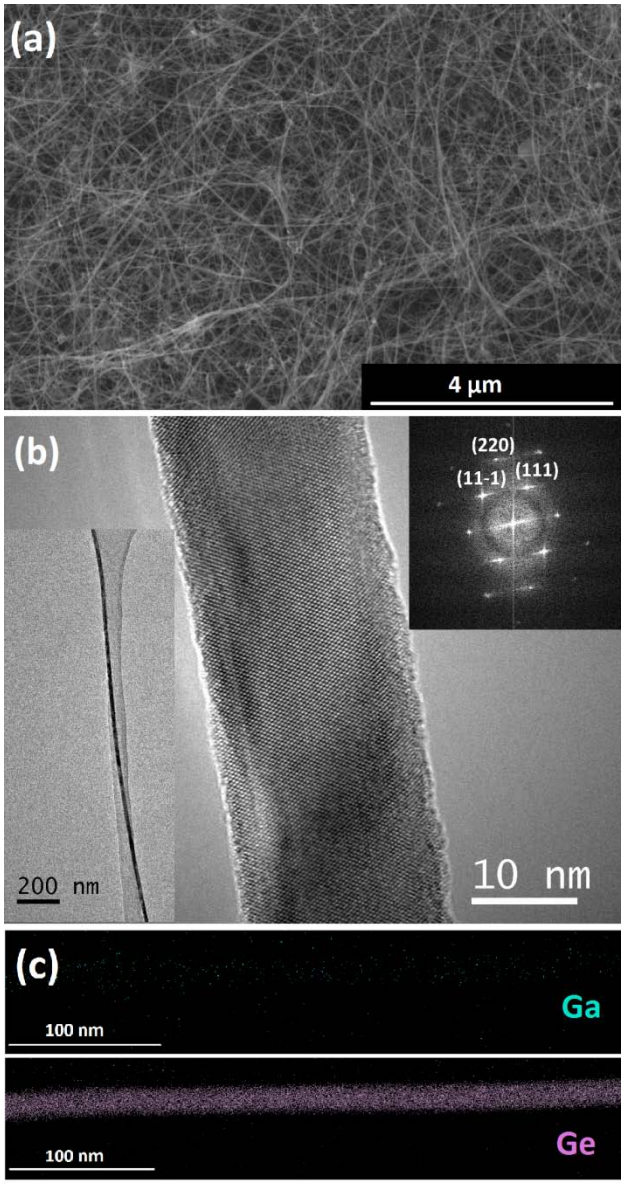

Figure 2: (a) The SEM image shows a high density of thin Ge NWs grown at a temperature of 390 °C using predeposited Ga seeds. The High resolution TEM image in (b) reveals the high crystallinity of the Ge NWs and their ⟨110⟩ growth direction according to the related FFT pattern. The TEM image in the inset also shows no tendency of tapering along the growth axis. (c) Elemental maps for Ga and Ge show no accumulation of Ga in the Ge crystal according to this measurement technique.

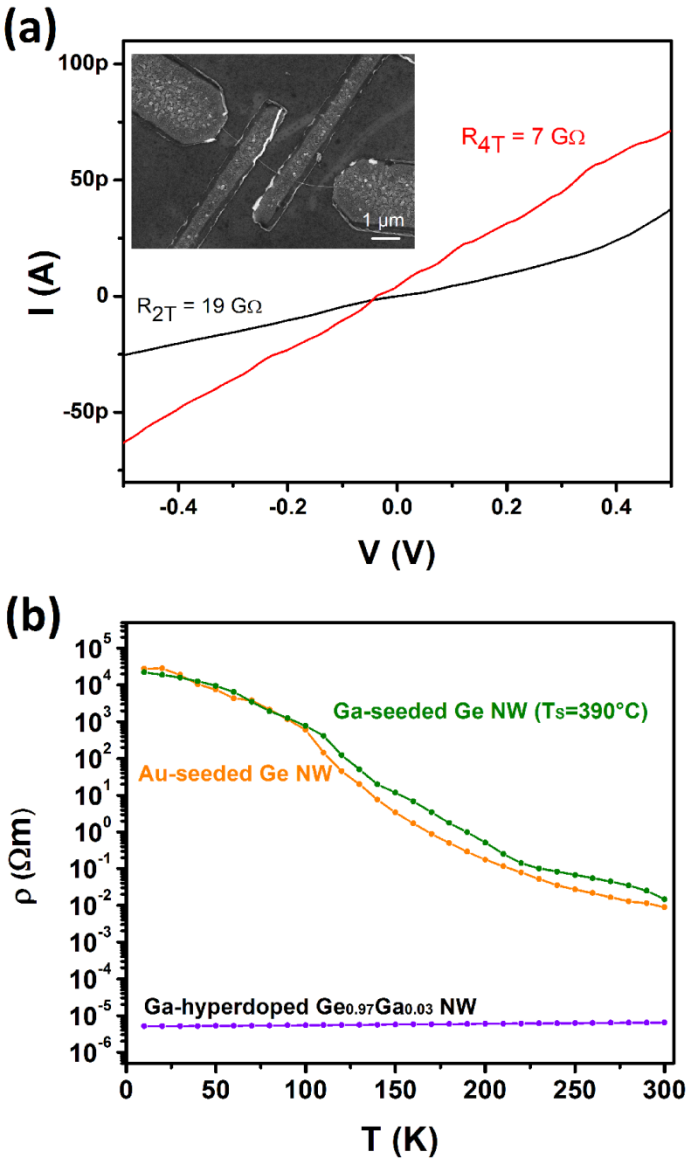

Figure 3. (a) I/V curves for a Ga-seeded Ge NW in two- and four-terminal geometry. The resistance values have been obtained from the linear region in the low bias regime. (b) Temperature dependence of the resistivity illustrates a similar behavior as intrinsic Ge NWs grown by Au-seeding and a remarkable difference to Ga-hyperdoped Ge NWs described in literature.[12]

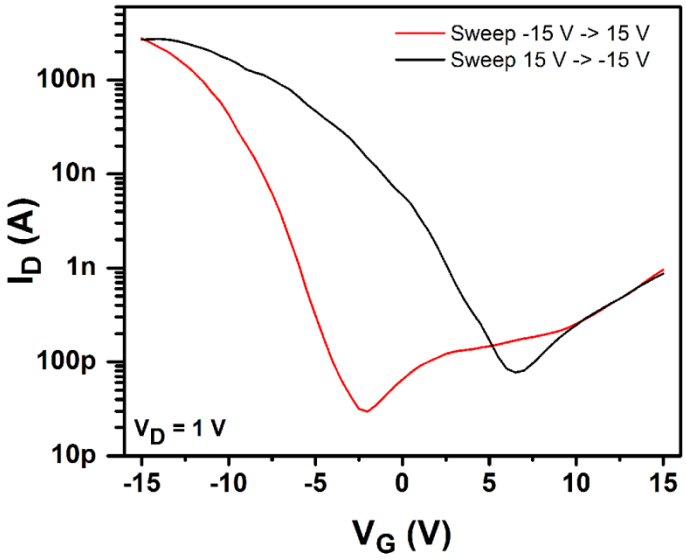

Figure 4 Transfer characteristics of a Schottky FET behavior consisting of a Ge NW contacted by Al pads on a silica dielectric layer showing voltage sweeps from different pre-polarisation.